

Predicting the start, peak and end of the Betula pollen season in Bavaria, Germany

A. Picornell, J. Buters, J. Rojo, Claudia Traidl-Hoffmann, Athanasios Damialis, A. Menzel, K. C. Bergmann, M. Werchan, C. Schmidt-Weber, J. Oteros

Angaben zur Veröffentlichung / Publication details:

Picornell, A., J. Buters, J. Rojo, Claudia Traidl-Hoffmann, Athanasios Damialis, A. Menzel, K. C. Bergmann, M. Werchan, C. Schmidt-Weber, and J. Oteros. 2019. "Predicting the start, peak and end of the Betula pollen season in Bavaria, Germany." *Science of The Total Environment* 690: 1299–309. <https://doi.org/10.1016/j.scitotenv.2019.06.485>.

Predicting the start, peak and end of the *Betula* pollen season in Bavaria, Germany

A. Picornell ^{a,*}, J. Buters ^b, J. Rojo ^{b,c}, C. Traidl-Hoffmann ^{d,e}, A. Menzel ^f, K.C. Bergmann ^g, M. Werchan ^g, C. Schmidt-Weber ^b, J. Oteros ^b

^a Department of Botany and Vegetal Physiology, University of Malaga, Campus de Teatinos, Malaga s/n, E-29071, Spain

^b Center of Allergy & Environment (ZAUM), Member of the German Center for Lung Research (DZL), Technische Universität München/Helmholtz Center, Munich, Germany

^c University of Castilla-La Mancha, Institute of Environmental Sciences, Toledo, Spain

^d Institute of Environmental Medicine (UNIKA-T), Technische Universität München, Munich, Germany

^e Center for Allergy Research and Education (CK-CARE), Davos, Switzerland

^f Technische Universität München, Ecoclimatology, Department of Ecology and Ecosystem Management, Freising, Germany

^g Foundation German Pollen Information Service (PID), Berlin, Germany

HIGHLIGHTS

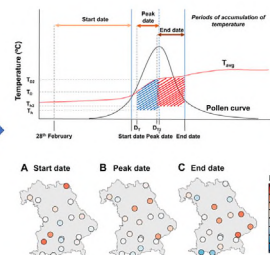
- Temperatures above 10 °C from February induce *Betula* flowering.
- Photoperiod is the main factor affecting the start of the forcing period.
- The peak and end of the pollen season are set by a heat accumulation from the start.

GRAPHICAL ABSTRACT

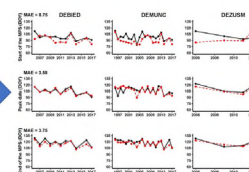
1. Pollen monitoring



2. Modelling



3. Forecast



* Corresponding author at: Departamento de Botánica y Fisiología Vegetal, Universidad de Málaga, Campus de Teatinos s/n, Málaga, E-29071, Spain.
E-mail address: picornell@uma.es (A. Picornell).

1. Introduction

Betula (birch) is a genus of woody plant species whose pollen is common in the atmosphere of central and northern regions of Europe, but are rare in the Mediterranean region (Beck et al., 2016). *Betula* genus in Bavaria is mainly represented by *Betula pendula* Roth and *Betula pubescens* Ehrh. (GBIF, 2019; Tutin et al., 1964). *Betula* pollen has been reported to cause severe allergic reactions in a high percentage of the European population (Burbach et al., 2009; Estrella et al., 2006; European Academy of Allergy and Clinical Immunology, 2015, 2014). For these reasons, models to predict the start, peak and end date of the Main Pollen Season (MPS) would be useful for allergic individuals to better manage their allergic disease.

Airborne pollen concentrations are highly influenced by meteorological variables, and temperature is the dominant variable for flower development and pollen release (Caffarra et al., 2011a; Chuine, 2000; Chuine and Cour, 1999; Jato et al., 2002; Laaidi, 2001; Linkosalo et al., 2010; Recio et al., 2018; Rodríguez-Rajo et al., 2003).

The majority of woody plant species in temperate zones have adapted to cold climate conditions during winter by inducing themselves in a physiological state of rest called dormancy (Lang et al., 1987). To break dormancy and to induce flowering, two conditions are necessary: a period of low temperatures (chilling period) followed by a period of relatively warm temperatures (quiescence) in which temperatures are accumulated to initiate bud growth. Once the buds are formed, a certain temperature accumulation is necessary (forcing) for budburst (Chuine, 2000; Kramer, 1994; Rodríguez-Rajo et al., 2003).

Several authors have modelled the start of the MPS for some pollen types (including *Betula*) in different parts of the world by using different techniques (such as temperature-based models, source-based models, logistic additive models or numerical models based on different meteorological variables) (Cotos-Yáñez et al., 2004; Emberlin et al., 1993; Estrella et al., 2006; García-Mozo et al., 2008; Linkosalo et al., 2010; Pfaar et al., 2017; Recio et al., 2018; Rodríguez-Rajo et al., 2003; Skjøth et al., 2007; Spieksma et al., 1995). Nevertheless, birch populations from different areas show different thermal requirements to flower due to adaptation to local conditions. Consequently, the optimal parameters of the numerical models to predict the occurrence of the phenological stages can change widely at different regions (Chuine and Cour, 1999; Jato et al., 2002). In addition, models to forecast the peak and end date were less frequently developed but these parameters are relevant to determine the length and intensity of the pollen season of birch.

Using these models, future changes in airborne pollen patterns due to climate change can be estimated by modelling the relationship between temperature and the flowering timing (Cecchi et al., 2010; Tormo-Molina et al., 2010; Van Vliet et al., 2002).

The main aim of this study was the development and validation of models for predicting the start, peak and end date of the main pollen season of *Betula* in Bavaria, Germany. These forecasting models can support the allergic population, provide information to estimate the impacts of climate change on reproductive plant development, and estimate the development of allergic pollen exposure in the future.

2. Material and methods

2.1. Monitoring sites

The study was conducted using 26 locations in Bavaria, a state in the southeast of Germany (see Appendix A): Altötting (DEALTO), Augsburg (DEAUGS), Bamberg (DEBAMB), Bayreuth (DEBAYR), Berchtesgaden (DEBERC), Biederstein-Munich (DEBIED), Donaustauf (DEDONA), Erlangen (DEERLA), Feucht (DEFEUC), Gaißach (DEGAIS), Garmisch-Partenkirchen (DEGARM), Hof (DEHOF), Kitzingen (DEKITZ), Kösching (DEKOES), Landshut (DELANDS), Marktheidenfeld (DEMARK), Mindelheim (DEMIND), Munich (DEMUNC), Münnerstadt (DEMUST), Oettingen (DEOETT), Passau (DEPASS), Oberjoch (DEOBER), Trostberg (DETROS), Viechtach (DEVIEC), Weiden (DEWEID) and Zusmarshausen (DEZUSM). Bavaria is the biggest state of Germany and pollen forecasting of the area is complex due to large heterogeneity in terms of topography, climate conditions and vegetation distribution. Annual rainfall is also heterogeneously distributed in the area, i.e. is maximal in the Alpine region (Oberjoch, 1271 m a.s.l. with an average annual total precipitation of 1549 mm; reference period 1975–2017) and minimal in the north-west area (Kitzingen, 241 m a.s.l. with an average annual total precipitation of 581 mm; reference period 1975–2017). For the study locations, the annual mean temperature is maximal in the north-west and south-central area (Kitzingen, 241 m a.s.l. with an average annual mean temperature of 9.84 °C and Munich, 522 m a.s.l. with 9.80 °C; reference period 1975–2017) and minimal in the Alpine region and in the north-east (Oberjoch, 1271 m a.s.l. with an average annual mean temperature of 7.17 °C and Hof, 523 m a.s.l. with 7.20 °C; reference period 1975–2017) (Oteros et al., 2018).

2.2. Meteorological data

Meteorological datasets of each station were obtained from E-OBS database (Cornes et al., 2018) (Appendix B). For each pollen sampling station, the nearest meteorological station was selected. Only meteorological stations with complete datasets for the studied period were considered. The maximum distance between meteorological station and pollen station was 17 km, and the mean distance was 6 km. Daily average temperature (obtained according to the Deutscher Wetterdienst standard procedure) was extracted for each day of the studied period (Haylock et al., 2008).

2.3. Pollen data

Airborne pollen was collected using Hirst-type volumetric traps (Hirst, 1952). The pollen traps sampled at a continuous flow of 10 l/min. Samples were mounted according to the methodology proposed by the European Aerobiology Society (Galán et al., 2014). From each slide, 4 longitudinal transects (>7% of the total surface) were counted in 12 h intervals, according to the methodology proposed by the German Pollen Information Service Foundation (PID) (Winkler et al., 2001) and the recommendations of the VDI (VDI4252-4, 2016). Pollen data were expressed as daily average concentrations (pollen/m³).

The start and end date of the main pollen season (MPS) were determined by the 5%/95% criterion (Nilsson and Persson, 1981) to avoid long

tails in the pollen curve and to exclude pollen detected from long term transport. The start date was defined as the day in which the accumulated value of pollen reached the 5% of the Annual Pollen Integral and the end date was the day in which the accumulated value reached the 95% of the Annual Pollen Integral. The peak date was the day when the maximum concentration of pollen was detected for each year. Data were managed with the “AeRobiology” R package (Development-Core-Team, 2017; Rojo et al., 2019).

Pollen daily concentrations of the year 2015 were used as training datasets for the models and for the internal validation. As observed in Appendix B, the average mean temperature and precipitation of the year 2015 was near to the mean values (1975–2017) in most stations for the months of February–May. Only good quality datasets were taken into account during the training process: datasets of stations with missing peaks (missing data within two days close or on to the day of maximum value), stations with >20% of missing data within the MPS, or stations whose start, peak or end dates of the MPS were considered as outliers ($z\text{-scores} > |2|$) were not included in the training process. After the filtration process, 19 stations were used to train the models: DEALTO, DEAGUS, DEBIE, DEDONA, DEFEUC, DEGAIS, DEGARM, DEHOF, DEKITZ, DEKOE, DEMARK, DEMIND, DEMUNC, DEOBER, DEOETT, DEPASS, DETROS, DEVIEC, DEWEID (see Appendix C).

2.4. Validation of the models

For the start, peak and end dates of the MPS different models were elaborated. Each model was trained with the same datasets and their predictions, expressed as dates, were compared to the real dates. The best models were chosen according to the Mean Absolute Error (MAE) (Eq. 1) obtained in its internal validation. MAE proved to be less unambiguous and more easily interpretable than the Root Mean Square Error (RMSE) in assessing average model performance (Willmott and Matsuura, 2005).

$$MAE = \frac{\sum_{i=1}^n |Predicted - Observed|}{n} \quad (1)$$

where n , number of cases; *Predicted*, the predicted date by the models; *Observed*, the observed date.

The models were externally validated with the historical time series of DEBIE station (years 2006–2017, excluding 2015 which was used as training dataset), DEMUNC station (years 1996–2017, excluding 2015 which was used as training dataset) and DEZUSM station (years 2006, 2009, 2011 and 2012; station not included in the training process). For the external validation, the bias of the models prediction was corrected with the internal error of the model for the target station.

2.5. Model for predicting the start of the MPS

The model was based on Chuine state of forcing Eq. (2) (Chuine, 2000), which was initially developed to predict the necessary sum of heat to initiate bud growth. The results are expressed as forcing units, which are non-dimensional and can be understood as a mathematical transformation of heat (Chuine and Cour, 1999).

$$Sf = \sum_{F1}^F \frac{1}{1 + e^{d(T_{avg} - c)}} \quad (2)$$

where Sf the state of forcing, $F1$ the forcing period start date, F the start of the main pollen season, d a numeric parameter with

negative values, T_{avg} the daily average temperature and c the temperature threshold. The state of forcing is the sum of heat which is necessary to detonate the start of the main pollen season. Results are expressed in forcing units. If the average temperature of a day overpasses the temperature threshold, this day has a big contribution to the state of forcing, i.e., a high number in the equation. If the average temperature of a day is under the threshold, its temperature also contributes to the state of forcing but having very low impact, i.e. a low number in the equation.

To choose the best model, different values of each parameter were tested. For c the temperatures between 0 °C and 18 °C were tested. This range of temperatures was chosen according to the reasonable thresholds for the average daily temperature during this period of the year. For d , values between −10 and 0 were tested. For the forcing period start date ($F1$), two different criteria were used: photoperiod and temperature. For photoperiod, different Julian days since 15th December of the previous year until 1st March of the current year were tested. Later dates imply more sun hours within a day. For temperature, two different methods were tested: the day in which a change in the daily average temperature trend was observed for each station (i.e., when temperature starts increasing); and the first day, since the day selected with the previous method (change in the daily average temperature trend), in which the daily average temperature exceeded a certain threshold (with thresholds from 0 °C to 12 °C with a resolution of 1 °C). This range of temperature was selected according to the reasonable thresholds for the average daily temperature during this period of the year (cooler than the forcing period). The day of the mentioned trend change was selected by doing a moving mean of the daily average temperature with a window size of 5 days, and selecting the moving mean in which the minimum value was observed. The date within that 5-days window which showed the smallest daily average temperature was chosen. The model with the combination of parameters that obtained the minimum MAE during its internal validation was selected.

For the optimization of the parameters, Nelder & Mead algorithm was used to simultaneously optimize $F1$, d and c parameters (Nelder and Mead, 1965). With the values obtained, manual “one by one” optimization was performed to ensure that the optimization algorithm did not select a local minimum (i.e., the values of two of the variables were fixed in the minimum found by the algorithm while testing different values of the third variable). For this second optimization, steps of 1 °C were tested for c , steps of 0.25 were tested for d , and all forcing period start dates selected with the criteria mentioned above were tested.

2.6. Model for predicting the peak and end of the MPS

These models assume that the flowers are already formed at the start of the MPS, but optimal temperature conditions are necessary to induce pollen release (Clot, 2001; Hicks et al., 1994; Subba Reddi and Reddi, 2009): the optimal conditions for the opening of anthers in the peak model, and the optimal conditions for the total liberation of pollen in the end model. All the elaborated models were based in the accumulated heat above a certain threshold (“temperature threshold”, T_h) since the first day of the MPS in which a certain threshold is reached by the daily average temperature (“day threshold”, T_D) (3).

$$Heat = \sum_{D_T}^D (T_{avg} - T_h) \quad (3)$$

where D_T is the first day of the MPS that reaches the day threshold (T_D), D target date (peak date for the peak model and end date for

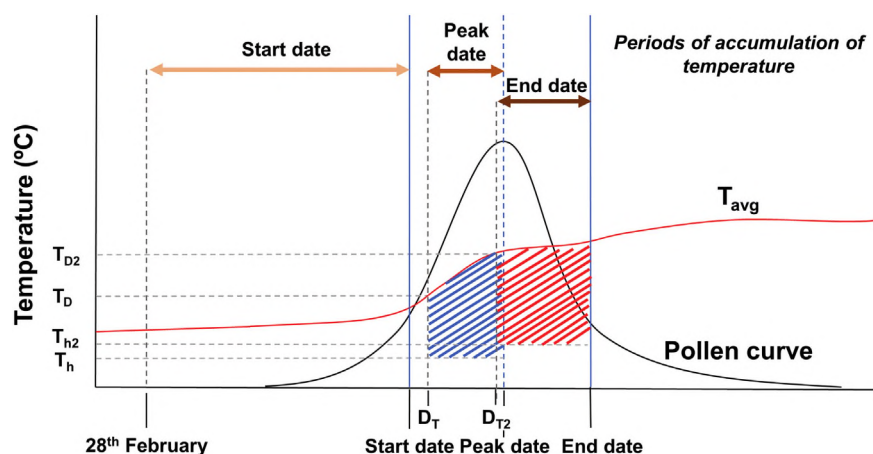


Fig. 1. Theoretical diagram of heat accumulation for each model. The area in blue represents the accumulated heat for the peak model, and the area in red the accumulated heat for the end model. The period in which temperature is accumulated for each model is marked with arrows in the upper part of the figure. T_D , day threshold for the peak model; T_{D2} , day threshold for the end model; D_T , the first day of the MPS that reaches the day threshold (T_D) for the peak model; D_{T2} , the first day of the MPS which reaches the day threshold (T_{D2}) for the end model; T_{avg} , daily average temperature; T_h , temperature threshold for the peak model; T_{h2} , temperature threshold for the end model. (For interpretation of the references to colour in this figure legend, the reader is referred to the web version of this article.)

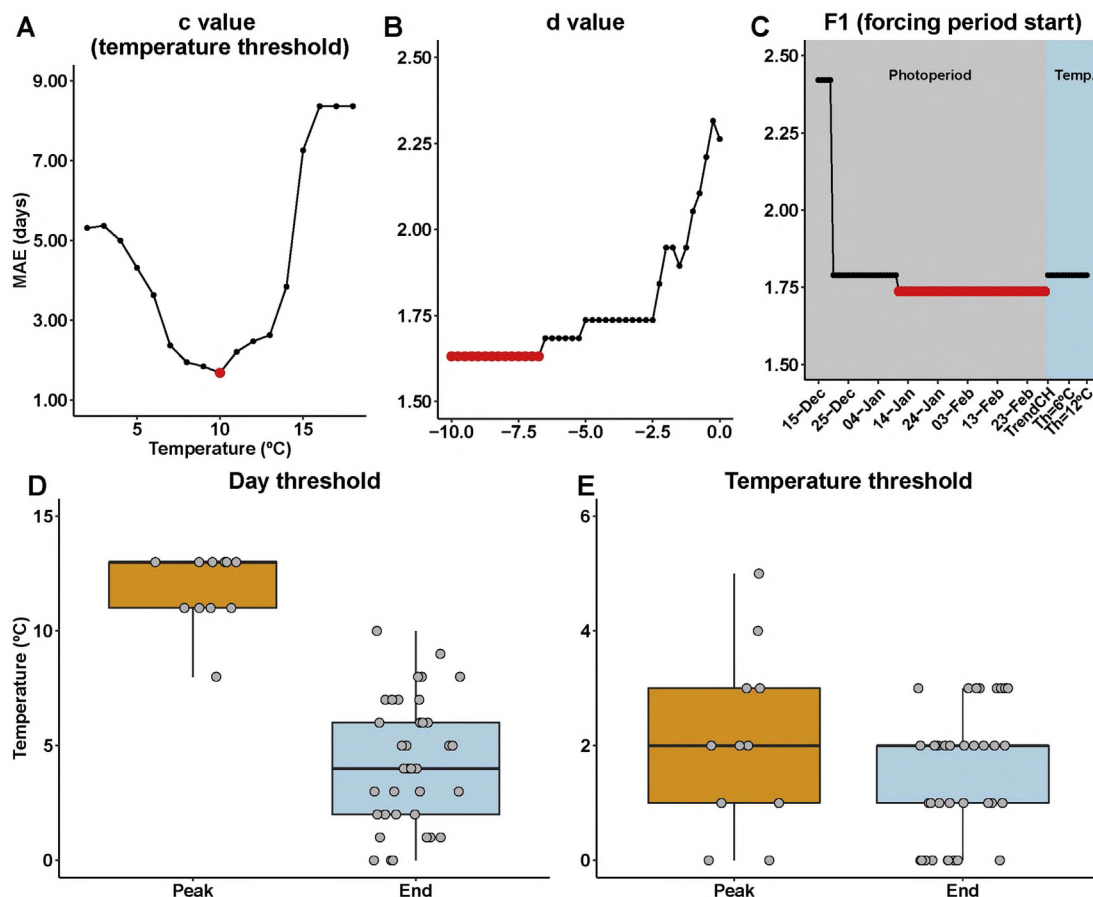


Fig. 2. Optimization of the models parameters. (A, B & C) Mean Average Error (in days) obtained from the training process of the start model by selecting different values for each parameter with the other parameters fixed in their optimal values (see Eq. 2). Optimal values are marked in red. (C) The dates to test for the F1 parameter were selected according to two different criteria: photoperiod (grey) and temperature (blue). For photoperiod, different Julian days since 15th December of the previous year until 1st March of the current year were tested. For temperature two different methods were tested: the day in which a change in the daily average temperature trend was observed for each station ("Trend CH"); and the first day, since the day selected with the previous method, in which the daily average temperature exceeded a certain threshold (with thresholds from 0 °C to 12 °C, with a resolution of 1 °C; $T_h = 0$ °C–12 °C). (D) Pool of all the "day thresholds" selected for the peak and end models. The "day thresholds" are the thresholds of temperature (in °C) which determine the day in which the accumulation of heat starts. They are used to mark the first day of the main pollen season whose daily average temperature exceeds the threshold. (E) Pool of all the "temperature thresholds" selected for the peak and end models. Only temperatures over the temperature thresholds are taken into account for the accumulation of temperature of the models (see Eq. 3). Boxes in D and E include the 50% of the data. Points in grey represent parameters of each individual model which is part of the pool of models (orange for the peak model and blue for the end model). (For interpretation of the references to colour in this figure legend, the reader is referred to the web version of this article.)

the end model), T_h the temperature threshold and T_{avg} the daily average temperature. Only temperatures above T_h are taken into account for the heat accumulation.

For each target date, models with all possible combination of the values of T_h (0–20 °C, resolution of 1 °C) and T_D (0–20 °C, resolution of 1 °C) were elaborated. These ranges of temperature were selected according to the reasonable thresholds for the average daily temperature during this period of the year (warmer than the forcing period). All the models with a MAE minor to the minimum MAE+0.25 were selected to make an assembly model. The weights of each model in the final assembly were established according to the z-score value of their prediction, i.e., models with a low z-score were given a higher weight in the final assembly.

The heat accumulation dynamics of each model are visually explained in Fig. 1. Each period of accumulation and the temperature accumulated are marked for each model.

2.7. Geographical representation of the models error

The errors obtained during the internal validation of the models were spatially represented to observe the accuracy by region. Data were processed by R software (Development-Core-Team, 2017) with a combination of different R packages: “sp”, “raster”, and “ggplot2” (Hijmans and van Etten, 2014; Pebesma and Bivand, 2005; Wickham, 2016).

3. Results and discussion

3.1. Models parametrization

The results obtained during the parametrization of the models are shown in Fig. 2.A, 2.B and 2.C. The optimal values of each parameter which were the closest to the initial Nelder & Mead optimization were chosen: –6.75 for d , 10 °C for c and 28th February for $F1$.

The optimal threshold for the start date model was set at 10 °C (Fig. 2.A). Temperatures above this value have a bigger impact in the state of forcing than temperatures below (see Eq. 2). Previous experimental studies carried out in central Europe (including Germany) for birch species, coinciding with our results, set the upper threshold for dormancy temperatures between 10 and 15 °C and proved that exposure to a constant temperature of 10 °C triggered dormancy release (Caffarra et al., 2011b, 2011a). Other previous study also set the threshold temperature to detonate flowering in birch in 10 °C, despite using a different methodology to accumulate heat (Clot, 2001).

High negative values of d parameter are optimal as shown in Fig. 2.B. Days with different temperatures above the c threshold are taken into account with almost the same weight (the result of Eq. 2 for these days is near 1 forcing unit) and days under the threshold are taken into account with almost the same weight (the result of Eq. 2 for these days is near 0 forcing units). d values in the literature change widely according to the species and to the geographical area, but always took negative values (Caffarra et al., 2011a, 2011b; Chuine, 2000; Chuine et al., 1999). According to these results, birch flower maturation and pollen release might be conditioned by hot days at the beginning of spring as suggested by a previous study (Clot, 2001). Cold days would not have relevance for the heat accumulation process, and they will not increase the amount of heat needed to detonate the main pollen season. Therefore, they only are able to delay the fulfilment of the forcing requirements.

Temperature criteria for determining the forcing period start ($F1$) produced bigger errors than the photoperiod criteria (Fig. 2.C). Therefore, the trigger signal to start the accumulation of heat should be more related to photoperiod than to temperature. Other authors, in accordance with our results, have described photoperiod

as one of the main factors which control the timing of phenophases in several tree species (including *Betula* species). Some of them have concluded that photoperiod affects the growth initiation in *Betula* species and that it presents an interaction with temperature (Caffarra et al., 2011a, 2011b; Clot, 2001; Heide, 1993; Linkosalo et al., 2010; Myking and Heide, 1995; Sofiev et al., 2013; Thomas and Vince-Prue, 1997). According to the model obtained, the photoperiod of the days near the 28th February sets the onset of the heat accumulation process to detonate the start of the main pollen season of *Betula*. Temperatures of March and April are critical to determine the start date and 3.96 ± 1.88 forcing units must be accumulated as forcing requirements (Eq. 2) to detonate the start of the birch MPS. Coinciding with our results, other temperature-based studies of *Betula* phenology have also concluded similar dates to set the start of the heat accumulation process in Europe (1st March or 4th March for some species) and even found significant correlations between February–April temperatures and budburst dates (Clot, 2001; Donnelly et al., 2006; Linkosalo et al., 2010; Sofiev et al., 2013). Cold periods during the end of March or the beginning of April will cause a delay in the start of the MPS since the forcing units needed to detonate flowering are usually reached during these days.

The “day threshold” and “temperature threshold” values selected for the models are shown in Fig. 2.D & 2.E respectively. For the peak, there is a clear “day threshold” to mark the start of the heat accumulation process between 11 and 13 °C for the daily average. A day with temperatures above these thresholds is necessary to trigger the heat accumulation for the peak. For the end model, there is a huge variability of temperatures selected between 0 and 10 °C as “day thresholds”. For our training dataset, all these thresholds are reached during the first day of the main pollen season. It could mean that the accumulation of heat to detonate the end starts always on the start date of the main pollen season or on a date near it.

For the “temperature thresholds” all values for both models were between 0 and 5 °C for the peak model and between 0 and 3 °C for the end model. Since there were no days between these ranges of temperature in the training datasets, all the models with temperatures between these ranges perform the same prediction, i.e., all the heat above 0 °C is taken into account for the accumulation process. A heat accumulation over the temperature threshold of approximately 45.36 ± 12.31 °C is necessary to detonate the peak and 149.64 ± 18.46 °C to determine the end of the MPS of birch. For more details about the heat accumulation process, consult Fig. 1.

The presented results suggest that the duration of the MPS, which is determined by the end date for a given start date, is mainly influenced by temperatures during the MPS. These observations may suggest that, according with our previous hypothesis, the end of the MPS would be related to conditions favouring the pollen emission and not to conditions favouring the pollen production and flower development.

Other models were also tested to predict the start, peak and end dates, e.g., number of days with a daily average temperature above a certain threshold, number of days since the first day in which a certain temperature threshold was overpassed, accumulated heat since the day in which a relative maximum in the daily average temperature was detected, the previous models but replacing the daily average temperature with the moving mean of this variable (with 3, 5, 7 and 9 days of moving mean), and also making separate models for groups of stations obtained by clustering according to their annual mean temperature and other climate variables provided by Worldclim (Fick and Hijmans, 2017): mean diurnal range, isothermality, temperature seasonality, maximum temperature of the warmest month, minimum temperature of the coldest month, temperature annual range, mean temperature of the wettest quarter of the year, mean temperature of the driest quarter of the

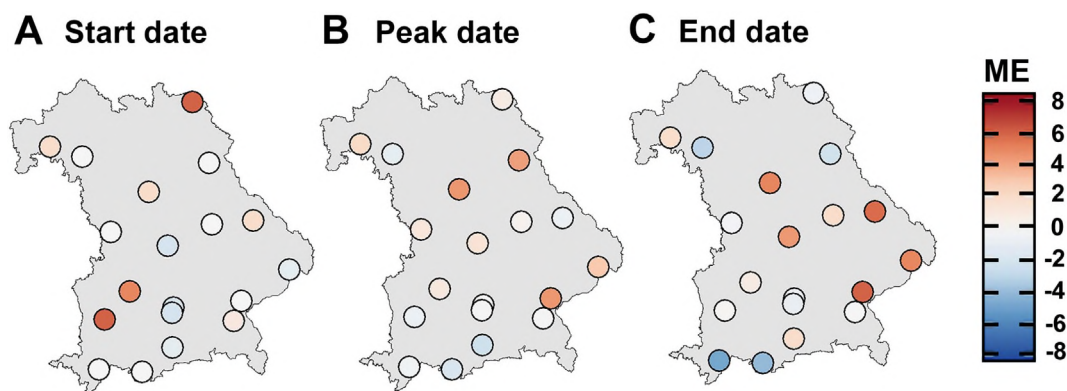


Fig. 3. Spatial representation of the models errors (ME) for the whole area of Bavaria. Based on the error obtained from the internal validation by station (points). Negative values represent early predictions and positive values late predictions.

year, mean temperature of the warmest quarter of the year, mean temperature of the coldest quarter of the year, annual precipitation, precipitation seasonality (different clustering methods were also tested). For the start model, the same model used for the peak date and for the end of the MPS was also tested. Nevertheless, the best fitted models were the ones selected and described in this manuscript.

3.2. Geographical interpolation of the models error

The maps obtained are shown in Fig. 3. These maps are just a first approximation to the error expected in these areas but help to visualize the errors obtained in each station during the internal validation. The geographical areas with a highest error in the start model (Fig. 3.A) are the areas surrounding DEMIND, DEAGS and DEHOF stations. DEMUNC, DEBIE and DEKOE have also larger errors in their predictions than the average. For the peak and end models (Fig. 3.B and .C), the errors are more homogeneously distributed. They are mostly concentrated in high and cold areas (Alpine and Bavarian forest areas). It could be explained as the result of the adaptation of birch populations to extreme conditions, producing a singular biological behaviour regarding to the rest of the geographic locations. These singularities are predicted by the models with less accuracy than the rest of locations. For better predictions for these areas, regional models could be designed in future studies.

The MAE obtained in the internal validation was 1.68 days for the start, 1.61 days for the peak and 2.61 days for the end.

3.3. External validation of the models

The MAE obtained in the external validation was 8.75 days for the start date, 3.58 days for the peak and 3.75 days for the end (see Fig. 4). It is remarkable that the highest external error was obtained in the model for the start of the season. It should be noted that the external locations used for the validation of the start model are located in the areas where highest internal error were observed (Fig. 3). For most of the region of Bavaria, lower external errors are expected.

Within the external validation error, other errors of the methodology are also integrated. Depending on the method used to define the start and end date of the MPS, dates can change or have different patterns of variations among years. The delay between flowering and pollen detection and the variability in local pollen concentrations produced by pollen from non-local areas also introduce small variations in the models performance. Long-term

transport of *Betula* pollen has been reported in other European countries at the beginning or the end of the MPS due to differences in phenology timing among distant areas (Skjøth et al., 2007). This effect has been minimized in the proposed models under normal conditions by using a restrictive percentage for establishing the MPS (i.e. the 90% definition of MPS excludes sporadic low amounts of pollen detected at the beginning or end of the season).

There are some years whose errors in the start model are bigger than for the rest of the years in the same location (2006 and 2010–2012 in DEBIE; 1998–2003, 2005–2006 and 2010–2012 in DEMUNC; 2006 in DEZUM). Most of these years coincide in all locations. This phenomenon may have two different explanations: unusual *Betula* response to temperatures or unusual atmospheric and/or meteorological conditions. We are unable to test the first hypothesis since no direct phenological data is available for these years and locations. The second hypothesis may be related to long transport events with higher influence than usually. Additionally, there may be other variables with less influence over phenology but whose effect may be increased under certain conditions.

The flowering period of *Betula* was also modelled in previous studies. Despite other models having different methodological approximations, they showed similar errors in their external validation. Linkosalo et al. (2010) obtained RMSE of 3 days for the start date and 5 days for the end in Finland. Despite conceptually MAE and RMSE should not be directly compared, their values should be proximal (Willmott and Matsuura, 2005). Caffarra et al. (2011a) modelled the timing to budburst in *Betula pubescens* with standard deviations between 0.4 and 6 days. This higher accuracy may be explained by modelling a single species of *Betula* under controlled conditions (ex situ) and by comparing with direct measurement of flowering phenology, not with pollen concentrations.

Sofiev et al. (2013) implemented a birch emission model in SILAM (Sofiev et al., 2008) and obtained fitting errors for phenological phases between 8 and 9 days for Bavaria region after developing an emission model for the whole Europe. These errors may be explained by the large area of application of the model. It would be interesting for future studies to apply these models only to Bavaria region and to compare the results with the obtained from replacing the thermal time flowering model integrated in SILAM by the proposed thermal models. Furthermore, dispersion models such as COSMO-ART (Vogel et al., 2009) may be used to issue daily forecasts of pollen concentrations within the dates of the main pollen season established by the presented models.

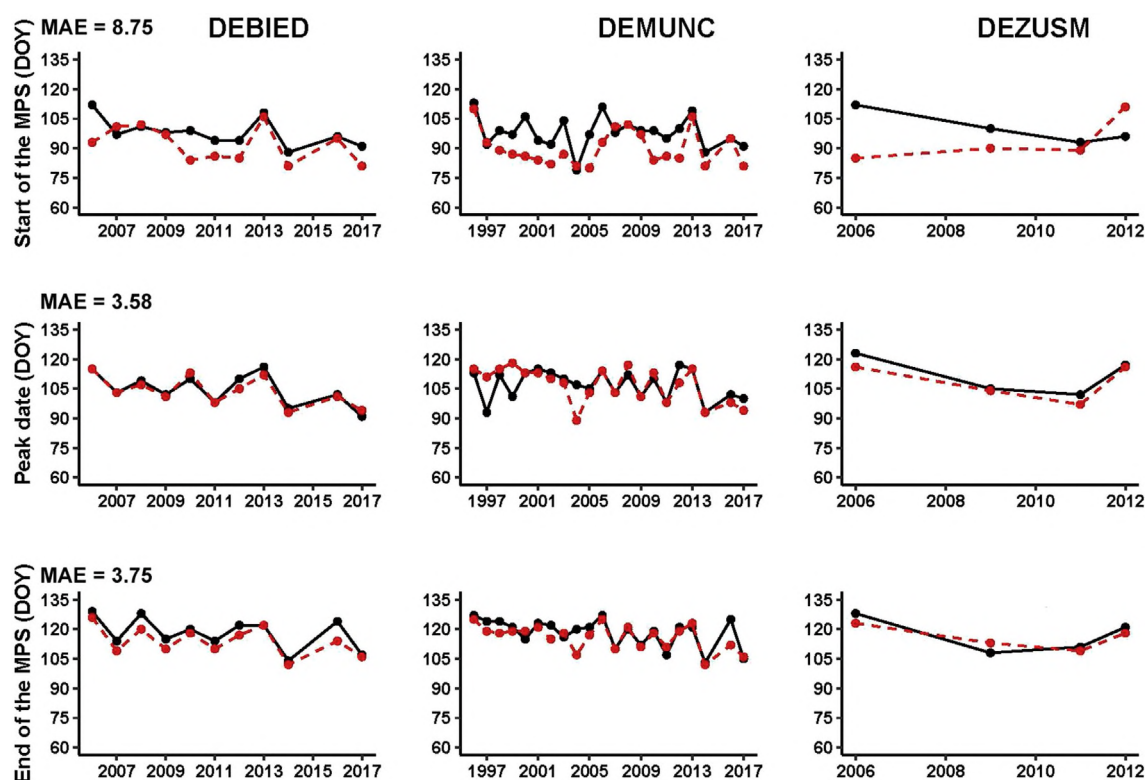


Fig. 4. External validation of the models. In red, the models prediction; in black, the observed dates. MAE: Mean average error of the models prediction for all the external validation datasets (in days). DOY: Day of the year. MPS: Main pollen season. The years of these stations used for building the model were excluded during the external validation. (For interpretation of the references to colour in this figure legend, the reader is referred to the web version of this article.)

Different models were developed for start, peak and end of the birch pollen season. The start date model was based on temperature accumulation after 28th of February onwards with a threshold of 10 °C (i.e. temperatures after 28th of February over 10 °C were the most relevant for the start of the season, before that date all temperatures were irrelevant). The peak prediction model uses the first day of the MPS in which 11–13 °C are reached as beginning point. Then all temperatures count. The end of the season uses the beginning of the pollen season as a starting point for the model. Then all temperatures count.

With the models obtained, start, peak and end dates of birch main pollen season can be estimated for the whole area of Bavaria by using meteorological forecasts as input data. With the relationships between temperature and phenological dates established in the models, changes in phenological dates due to climate change can be also estimated in future studies and the adaptability of the arboreal species as birch along an altitudinal gradient could be studied by intensification of the thermal-based phenological models in extreme climatic areas.

4. Conclusions

1. March–April temperatures were the most relevant for the start model (temperatures from the 28th of February onward) and 10 °C was set as the optimal threshold temperature. A heat accumulation of 3.96 ± 1.88 forcing units is needed to detonate the start of the MPS. The peak models take into account all temperatures accumulated since the first day of the main pollen season in which >11 °C is reached.
2. For the end of the main pollen season, the best fitted models were the ones which take into account all temperatures accumulated since the start of the main pollen season without a temperature threshold. Heat accumulations of 45.36 ± 12.31 °C and 149.64 ± 18.46 °C

(sum of temperature above 0 °C) are needed to detonate the peak and establish the end of the MPS respectively.

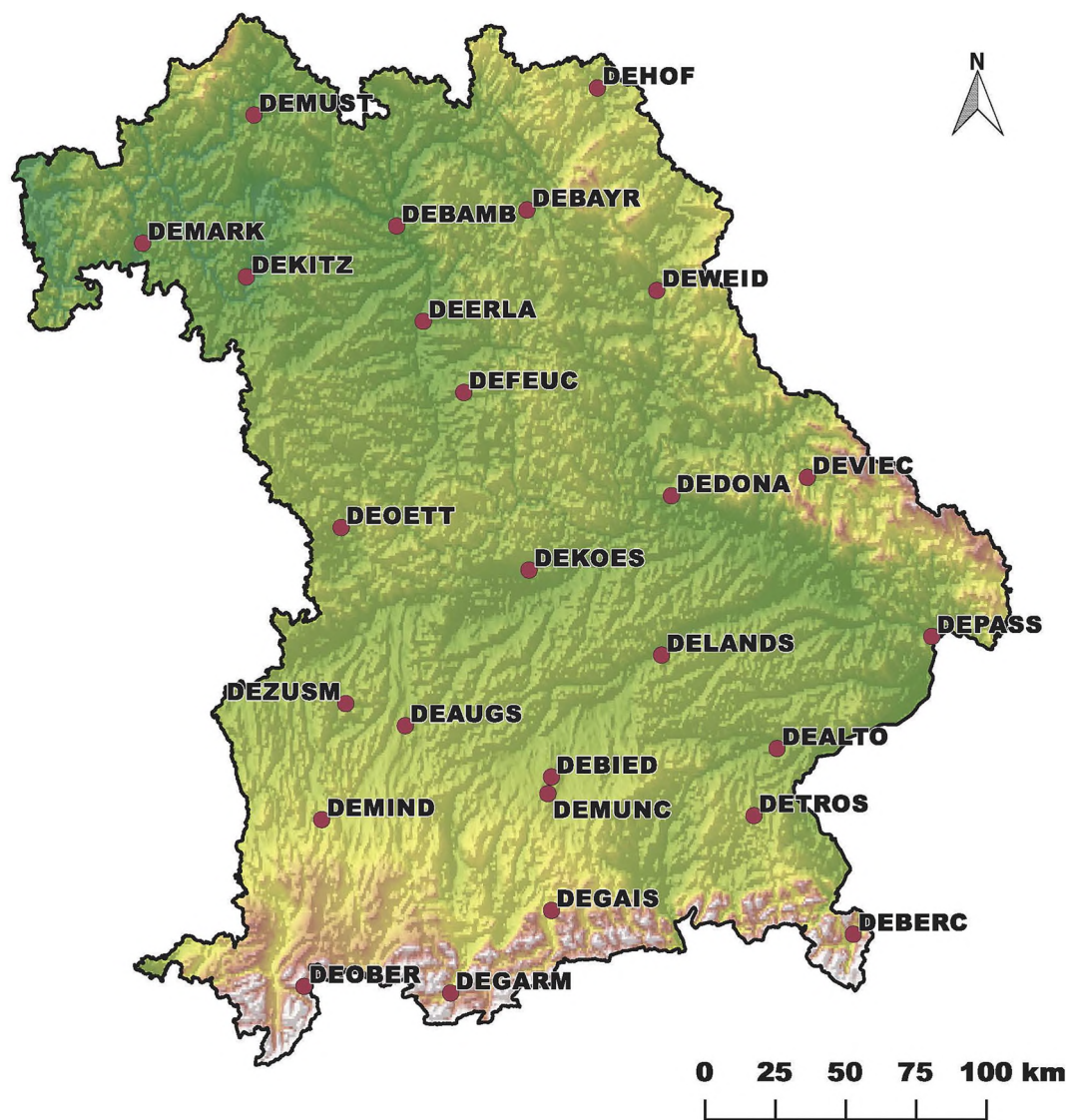
3. The models can predict with an external error of 8.75 days for the start, 3.58 days for the peak and 3.75 days for the end as average. The error in start of the season would add to the error for the other estimations if predicting before the start of the MPS.
4. With the models obtained, predictions of the start, peak and end of the main pollen season can be delivered to the pollen allergic population by using meteorological forecasts as input.
5. By means of the relationship established between temperatures and the pollen season, changes in the phenological behaviour of *Betula* species due to climate change can be estimated in future studies. According to the models delivered with Bavarian pollen databases, an increase in March–April temperatures due to climate change will cause an earlier start date of main pollen season of *Betula* in this area. The advance might be estimated in future studies by taking into account the different climate scenarios proposed by climate change studies.

Acknowledgements

This publication was funded by the Bavarian State Ministry of Health and Care grant G47-G8180.1-2014/5-25 and the Bavarian State Ministry of the Environment and Consumer Protection grant TKP01KPB-69312 and TKP01KPB-73815. A. Picornell was supported by a predoctoral grant financed by the Ministry of Education, Culture and Sports of Spain, in the Program for the Promotion of Talent and its Employability (FPU15/01668). J. Oteros was supported by a Postdoctoral grant of Helmholtz Zentrum Munich PFP III 2018-2020.

We acknowledge the E-OBS dataset for the EU-FP6 project ENSEMBLES (<http://ensembles-eu.metoffice.com>) and the data providers in the ECA&D project (<http://www.ecad.eu>).

Appendix A



Location of the pollen sampling stations in Bavaria. DEALTO: Altötting; DEAU: Augsburg; DEBAMB: Bamberg; DEBAYR: Bayreuth; DEBERC: Berchtesgaden; DEBIE: Munich-Biederstein; DEDONA: Donaustauf; DEERLA: Erlangen; DEFEUC: Feucht; DEGAIS: Gaißach; DEGARM: Garmisch-Partenkirchen; DEHOF: Hof; DEKITZ: Kitzingen; DEKOE: Kösching; DELANDS: Landshut; DEMARK: Marktheidenfeld; DEMIND: Mindelheim; DEMUNC: Munich; DEMUST: Münnerstadt; DEOETT: Oettingen; DEPASS: Passau; DEOBER: Oberjoch; DETROS: Trostberg; DEVIEC: Viechtach; DEWEID: Weiden; DEZUSM: Zusmarshausen. Plotted over topography map.

Appendix B. A Comparison of the mean average temperature and total precipitation of late winter and spring months between 2015 and historical data in each sampled station of Bavaria

Station	Month	Tavg 2015 (°C)	Mean Tavg (°C)	Prec. 2015 (mm)	Mean Prec. (mm)
DEALTO	February	−1.5	−0.1 ± 2.8	10.3	43.3 ± 26.4
DEALTO	March	5.0	4.2 ± 1.8	48.8	59.2 ± 34.5
DEALTO	April	8.6	8.3 ± 1.5	59.5	53.0 ± 30.0
DEALTO	May	13.5	13.4 ± 1.5	131.4	88.9 ± 39.8
DEAUGS	February	−1.4	0.3 ± 2.9	12.6	36.6 ± 20.5
DEAUGS	March	5.0	4.3 ± 1.9	33.6	45.5 ± 30.1
DEAUGS	April	8.4	8.1 ± 1.4	62.9	54.2 ± 30.9
DEAUGS	May	13.3	13.0 ± 1.5	102.5	84.0 ± 42.3
DEBAMB	February	0.4	0.9 ± 2.7	6.2	36.9 ± 22.6
DEBAMB	March	5.3	4.7 ± 1.8	32.0	46.7 ± 32.1
DEBAMB	April	8.5	8.7 ± 1.5	15.0	39.0 ± 20.6

(continued)

Station	Month	Tavg 2015 (°C)	Mean Tavg (°C)	Prec. 2015 (mm)	Mean Prec. (mm)
DEBAMB	May	13.6	13.7 ± 1.5	23.8	61.8 ± 37.2
DEBAYR	February	−0.5	0.2 ± 2.8	6.8	46.1 ± 29.2
DEBAYR	March	4.5	4.0 ± 1.9	48.1	53.2 ± 33.7
DEBAYR	April	7.7	7.9 ± 1.5	39.4	42.8 ± 21.6
DEBAYR	May	12.9	13.0 ± 1.5	21.2	61.4 ± 33.7
DEBERC	February	−0.9	0.5 ± 3.0	14.9	84.3 ± 56.0
DEBERC	March	4.9	4.6 ± 2.0	106.8	118.4 ± 71.3
DEBERC	April	8.8	8.6 ± 1.5	60.7	97.9 ± 65.5
DEBERC	May	13.3	13.3 ± 1.6	182.8	136.6 ± 60.6
DEBIED	February	−0.2	1.5 ± 2.9	19.5	45.0 ± 24.1
DEBIED	March	6.1	5.5 ± 2.0	66.1	60.6 ± 28.2
DEBIED	April	10.2	9.3 ± 1.6	62.1	65.0 ± 36.2
DEBIED	May	14.2	14.1 ± 1.6	135.5	100.6 ± 48.0
DEDONA	February	−0.6	0.2 ± 2.7	6.0	36.8 ± 21.2
DEDONA	March	5.7	4.7 ± 1.9	29.9	43.6 ± 29.2
DEDONA	April	9.2	9.2 ± 1.6	33.0	37.7 ± 21.4
DEDONA	May	13.7	14.2 ± 1.6	78.1	63.1 ± 31.0
DEERLA	February	0.4	0.7 ± 2.7	9.7	46.5 ± 24.7
DEERLA	March	5.7	4.5 ± 1.9	51.4	57.3 ± 41.2
DEERLA	April	9.0	8.7 ± 1.7	34.3	49.8 ± 27.8
DEERLA	May	14.0	13.8 ± 1.6	29.4	68.8 ± 40.5
DEFEUC	February	−0.8	0.4 ± 2.7	17.2	46.4 ± 26.0
DEFEUC	March	4.7	4.1 ± 1.9	39.3	53.1 ± 38.1
DEFEUC	April	7.6	8.0 ± 1.5	42.3	49.2 ± 27.2
DEFEUC	May	12.8	13.1 ± 1.6	51.8	73.4 ± 42.4
DEGAIS	February	−1.9	−0.5 ± 3.1	41.0	80.5 ± 43.7
DEGAIS	March	4.2	3.4 ± 2.2	81.3	99.5 ± 46.9
DEGAIS	April	8.4	7.6 ± 1.6	73.8	89.3 ± 40.2
DEGAIS	May	12.5	12.4 ± 1.6	247.1	138.2 ± 63.4
DEGARM	February	−2.1	−0.9 ± 2.5	26.2	65.3 ± 40.4
DEGARM	March	4.1	3.0 ± 2.0	81.4	92.2 ± 45.5
DEGARM	April	7.9	6.9 ± 1.7	85.2	92.0 ± 39.5
DEGARM	May	12.2	11.7 ± 1.5	233.6	132.1 ± 57.3
DEHOF	February	−1.3	−1.2 ± 2.9	9.3	45.6 ± 28.8
DEHOF	March	3.6	2.5 ± 2.2	47.8	51.2 ± 28.1
DEHOF	April	6.9	6.5 ± 1.8	44.2	44.9 ± 23.6
DEHOF	May	11.7	11.5 ± 1.6	18.1	61.0 ± 35.7
DEKITZ	February	1.1	1.7 ± 2.9	9.9	34.9 ± 21.5
DEKITZ	March	5.9	5.5 ± 1.8	41.4	40.1 ± 27.6
DEKITZ	April	9.8	9.8 ± 1.5	18.6	36.1 ± 21.9
DEKITZ	May	14.7	14.5 ± 1.7	18.1	55.4 ± 33.3
DEKOES	February	−1.3	0.0 ± 2.7	10.2	39.4 ± 20.3
DEKOES	March	5.7	4.2 ± 2.0	34.0	45.9 ± 33.4
DEKOES	April	9.1	8.4 ± 1.7	63.9	43.4 ± 22.6
DEKOES	May	13.4	13.3 ± 1.6	57.5	69.2 ± 35.7
DELANDS	February	−1.2	0.2 ± 2.7	14.3	39.6 ± 24.6
DELANDS	March	5.5	5.3 ± 2.1	37.3	36.7 ± 15.9
DELANDS	April	9.3	9.7 ± 1.6	58.3	49.2 ± 24.6
DELANDS	May	13.4	13.6 ± 1.3	155.1	98.5 ± 44.6
DEMARK	February	0.4	1.4 ± 2.2	14.0	51.0 ± 28.2
DEMARK	March	5.3	5.0 ± 2.0	49.3	52.2 ± 36.2
DEMARK	April	9.0	9.7 ± 1.9	23.0	36.7 ± 22.7
DEMARK	May	13.0	13.5 ± 1.4	18.4	74.2 ± 41.5
DEMIND	February	−3.2	−0.6 ± 2.9	36.8	63.7 ± 38.0
DEMIND	March	3.9	3.2 ± 2.1	79.7	74.1 ± 38.4
DEMIND	April	7.3	6.7 ± 1.5	82.8	79.3 ± 46.4
DEMIND	May	12.2	11.7 ± 1.6	189.0	107.4 ± 58.9
DEMUNC	February	−0.2	1.5 ± 2.9	19.5	45.0 ± 24.1
DEMUNC	March	6.1	5.5 ± 2.0	66.1	60.6 ± 28.2
DEMUNC	April	10.2	9.3 ± 1.6	62.1	65.0 ± 36.2
DEMUNC	May	14.2	14.1 ± 1.6	135.5	100.6 ± 48.0
DEMUST	February	0.3	1.0 ± 2.6	9.0	46.6 ± 32.5
DEMUST	March	5.2	4.9 ± 1.9	43.3	50.6 ± 31.0
DEMUST	April	9.0	8.8 ± 1.5	14.6	40.5 ± 22.3
DEMUST	May	13.0	13.3 ± 1.4	16.3	60.0 ± 31.3
DEOBER	February	−2.9	−0.6 ± 2.9	54.9	94.4 ± 50.7
DEOBER	March	3.3	2.7 ± 2.0	94.5	114.4 ± 47.7
DEOBER	April	6.8	6.6 ± 1.5	137.1	107.9 ± 50.3
DEOBER	May	11.7	11.3 ± 1.3	218.8	160.1 ± 70.7
DEOETT	February	−1.0	0.4 ± 2.9	7.5	34.3 ± 21.9
DEOETT	March	5.3	4.5 ± 1.9	33.1	39.6 ± 25.7
DEOETT	April	9.1	8.4 ± 1.5	28.2	41.2 ± 24.5
DEOETT	May	13.6	13.2 ± 1.5	66.3	68.0 ± 37.2
DEPASS	February	−0.6	0.4 ± 2.7	12.7	57.0 ± 30.4
DEPASS	March	5.3	4.5 ± 1.8	50.0	70.7 ± 48.4

(continued on next page)

(continued)

Station	Month	Tavg 2015 (°C)	Mean Tavg (°C)	Prec. 2015 (mm)	Mean Prec. (mm)
DEPASS	April	8.7	9.2 ± 1.7	56.0	48.6 ± 27.0
DEPASS	May	13.2	13.9 ± 1.2	139.3	94.3 ± 44.2
DETROS	February	−1.5	0.3 ± 2.9	16.8	56.9 ± 32.4
DETROS	March	4.9	4.5 ± 2.0	63.9	77.6 ± 40.8
DETROS	April	8.9	8.4 ± 1.6	50.8	70.9 ± 40.3
DETROS	May	13.0	13.4 ± 1.5	135.2	107.9 ± 45.8
DEVIEC	February	−1.6	−0.3 ± 2.7	16.4	44.2 ± 20.8
DEVIEC	March	4.1	3.7 ± 1.9	52.3	50.0 ± 23.8
DEVIEC	April	7.4	8.4 ± 1.7	31.6	50.7 ± 33.5
DEVIEC	May	12.1	12.5 ± 1.2	71.1	99.6 ± 43.5
DEWEID	February	−0.6	−0.3 ± 2.7	7.7	39.8 ± 24.3
DEWEID	March	4.9	3.7 ± 2.0	49.4	48.5 ± 31.4
DEWEID	April	8.0	7.8 ± 1.7	34.6	38.6 ± 20.9
DEWEID	May	12.9	12.8 ± 1.5	42.5	67.6 ± 35.1
DEZUSM	February	−1.2	0.5 ± 2.7	17.3	36.0 ± 19.3
DEZUSM	March	5.2	4.8 ± 1.7	31.0	43.4 ± 30.5
DEZUSM	April	9.0	8.7 ± 1.4	79.2	51.5 ± 27.9
DEZUSM	May	13.7	13.5 ± 1.5	101.1	76.4 ± 39.9

Tavg 2015: monthly mean of the daily average temperatures in 2015 by month and location. Mean Tavg: mean and standard deviation of the monthly means of daily average temperatures along the period 1975–2017 by month and location. Prec. 2015: monthly total precipitation in 2015 by month and location. Mean Prec.: mean and standard deviation of the monthly sum of total precipitation along the period 1975–2017 by month and location. DEALTO: Altötting; DEAUGS: Augsburg; DEBAMB: Bamberg; DEBAYR: Bayreuth; DEBERC: Berchtesgaden; DEBIED: Munich-Biederstein; DEDONA: Donaustauf; DEERLA: Erlangen; DEFEUC: Feucht; DEGAIS: Gaißach; DEGARM: Garmisch-Partenkirchen; DEHOF: Hof; DEKITZ: Kitzingen; DEKOES: Kösching; DELANDS: Landshut; DEMARK: Marktheidenfeld; DEMIND: Mindelheim; DEMUNC: Munich; DEMUST: Münnerstadt; DEOBER: Oberjoch; DEOETT: Oettingen; DEPASS: Passau; DETROS: Trostberg; DEVIEC: Viechtach; DEWEID: Weiden; DEZUSM: Zusmarshausen. Meteorological datasets of each station were obtained from E-OBS database (Cornes et al., 2018).

Appendix C. Main dates and duration of birch main pollen season at the stations used to train the models in 2015

Location	Start	Peak	End	Duration (days)
DEALTO	13 April 2015	16 April 2015	23 April 2015	10
DEAUGS	08 April 2015	16 April 2015	25 April 2015	17
DEBIED	13 April 2015	16 April 2015	27 April 2015	14
DEDONA	13 April 2015	17 April 2015	25 April 2015	12
DEFEUC	13 April 2015	17 April 2015	27 April 2015	14
DEGAIS	14 April 2015	22 April 2015	28 April 2015	14
DEGARM	13 April 2015	22 April 2015	04 May 2015	21
DEHOF	15 April 2015	21 April 2015	05 May 2015	20
DEKITZ	11 April 2015	16 April 2015	29 April 2015	18
DEKOES	13 April 2015	16 April 2015	23 April 2015	10
DEMARK	11 April 2015	15 April 2015	25 April 2015	14
DEMIND	08 April 2015	22 April 2015	27 April 2015	19
DEMUNC	13 April 2015	16 April 2015	27 April 2015	14
DEOBER	14 April 2015	22 April 2015	08 May 2015	24
DEOETT	13 April 2015	16 April 2015	28 April 2015	15
DEPASS	13 April 2015	16 April 2015	23 April 2015	10
DETROS	12 April 2015	17 April 2015	27 April 2015	15
DEVIEC	14 April 2015	21 April 2015	27 April 2015	13
DEWEID	15 April 2015	16 April 2015	05 May 2015	20

Main pollen season calculated according to 5%/95% criterion (Nilsson and Persson, 1981). DEALTO: Altötting; DEAUGS: Augsburg; DEBIED: Munich-Biederstein; DEDONA: Donaustauf; DEFEUC: Feucht; DEGAIS: Gaißach; DEGARM: Garmisch-Partenkirchen; DEHOF: Hof; DEKITZ: Kitzingen; DEKOES: Kösching; DEMARK: Marktheidenfeld; DEMIND: Mindelheim; DEMUNC: Munich; DEOBER: Oberjoch; DEOETT: Oettingen; DEPASS: Passau; DETROS: Trostberg; DEVIEC: Viechtach; DEWEID: Weiden.

References

- Beck, P., Caudullo, G., de Rigo, D., Tinner, W., 2016. *Betula pendula*, *Betula pubescens* and other birches in Europe: distribution, habitat, usage and threats. In: San-Miguel-Ayán, J., de Rigo, D., Caudullo, G., Houston Durrant, T., Mauri, A. (Eds.), *European Atlas of Forest Tree Species*. Publ. Off. EU, Luxembourg, pp. 70–73 <https://doi.org/10.2788/4251>.
- Burbach, G.J., Heinzerling, L.M., Edenharter, G., Bachert, C., Bindeslev-Jensen, C., Bonini, S., Bousquet, J., Bousquet-Rouanet, L., Bousquet, P.J., Bresciani, M., Bruno, A., Canonica, G.W., Darsow, U., Demoly, P., Durham, S., Fokkens, W.J., Giavi, S., Gjomarkaj, M., Gramiccioni, C., Haahela, T., Kowalski, M.L., Magyar, P., Muraközi, G., Orosz, M., Papadopoulos, N.G., Röhrl, C., Stingl, G., Todo-Bom, A., von Mutius, E., Wiesner, A., Wöhrl, S., Zuberbier, T., 2009. GA2LEN skin test study II: clinical relevance of inhalant allergen sensitizations in Europe. *Allergy* 64, 1507–1515. <https://doi.org/10.1111/j.1398-9995.2009.02089.x>.
- Caffarra, A., Donnelly, A., Chuine, I., 2011a. Modelling the timing of *Betula pubescens* budburst. II. Integrating complex effects of photoperiod into process-based models. *Clim. Res.* 46, 159–170. <https://doi.org/10.3354/cr00983>.
- Caffarra, A., Donnelly, A., Chuine, I., Jones, M.B., 2011b. Modelling the timing of *Betula pubescens* budburst. I. Temperature and photoperiod: a conceptual model. *Clim. Res.* 46, 147–157. <https://doi.org/10.3354/cr00980>.
- Cecchi, L., D'Amato, G., Ayres, J.G., Galan, C., Forastiere, F., Forsberg, B., Gerritsen, J., Nunes, C., Behrendt, H., Akdis, C., Dahl, R., Annesi-Maesano, I., 2010. Projections of the effects of climate change on allergic asthma: the contribution of aerobiology. *Allergy Eur. J. Allergy Clin. Immunol.* 65, 1073–1081. <https://doi.org/10.1111/j.1398-9995.2010.02423.x>.
- Chuine, I., 2000. A unified model for budburst of trees. *J. Theor. Biol.* 207, 337–347. <https://doi.org/10.1006/jtbi.2000.2178>.
- Chuine, I., Cour, P., 1999. Climatic determinants of budburst seasonality in four temperate-zone tree species. *New Phytol.* 143, 339–349. <https://doi.org/10.1046/j.1469-8137.1999.00445.x>.

- Chuine, I., Cour, P., Rousseau, D.D., 1999. Selecting models to predict the timing of flowering of temperate trees: implications for tree phenology modelling. *Plant Cell Environ.* 22, 1–13. <https://doi.org/10.1046/j.1365-3040.1999.00395.x>.
- Clot, B., 2001. Airborne birch pollen in Neuchâtel (Switzerland): onset, peak and daily patterns. *Aerobiologia (Bologna)* 17, 25–29. <https://doi.org/10.1023/A:1007652220568>.
- Cornes, R.C., van der Schrier, G., van den Besselaar, E.J.M., Jones, P.D., 2018. An ensemble version of the E-OBS temperature and precipitation data sets. *J. Geophys. Res. Atmos.* 123, 9391–9409. <https://doi.org/10.1029/2017JD028200>.
- Cotos-Yáñez, T.R., Rodríguez-Rajo, F.J., Jato, M.V., 2004. Short-term prediction of Betula airborne pollen concentration in Vigo (NW Spain) using logistic additive models and partially linear models. *Int. J. Biometeorol.* 48, 179–185. <https://doi.org/10.1007/s00484-004-0203-9>.
- Development-Core-Team, 2017. *R: A Language and Environment for Statistical Computing*.
- Donnelly, A., Salamin, N., Jones, M.B., 2006. Changes in tree phenology: an indicator of spring warming in Ireland? *Biol. Environ.* 106, 49–56. <https://doi.org/10.3318/BIOE.2006.106.1.49>.
- Emberlin, J., Savage, M., Woodman, R., 1993. Annual variations in the concentrations of betula pollen in the London area, 1961–1990. *Grana* 32, 359–363. <https://doi.org/10.1080/00173139309428965>.
- Estrella, N., Menzel, A., Krämer, U., Behrendt, H., 2006. Integration of flowering dates in phenology and pollen counts in aerobiology: analysis of their spatial and temporal coherence in Germany (1992–1999). *Int. J. Biometeorol.* 51, 49–59. <https://doi.org/10.1007/s00484-006-0038-7>.
- European Academy of Allergy and Clinical Immunology, 2014. *Global Atlas of Allergy (Zurich)*.
- European Academy of Allergy and Clinical Immunology, 2015. *Global Atlas of Allergic Rhinitis and Chronic Rhinosinusitis (Zurich (Switzerland))*.
- Fick, S.E., Hijmans, R.J., 2017. WorldClim 2: new 1-km spatial resolution climate surfaces for global land areas. *Int. J. Climatol.* 37, 4302–4315. <https://doi.org/10.1002/joc.5086>.
- Galán, C., Smith, M., Thibaudon, M., Frenguelli, G., Oteros, J., Gehrig, R., Berger, U., Clot, B., Brandao, R., 2014. Pollen monitoring: minimum requirements and reproducibility of analysis. *Aerobiologia (Bologna)* 30, 385–395. <https://doi.org/10.1007/s10453-014-9335-5>.
- García-Mozo, H., Chuine, I., Aira, M.J., Belmonte, J., Bermejo, D., Díaz de la Guardia, C., Elvira, B., Gutiérrez, M., Rodríguez-Rajo, J., Ruiz, L., Trigo, M.M., Tormo, R., Valencia, R., Galán, C., 2008. Regional phenological models for forecasting the start and peak of the Quercus pollen season in Spain. *Agric. For. Meteorol.* 148, 372–380. <https://doi.org/10.1016/j.agrformet.2007.09.013>.
- GBIF, 2019. GBIF: The Global Biodiversity Information Facility. [WWW Document]. <https://doi.org/10.15468/dl.f4zjgg>.
- Haylock, M.R., Hofstra, N., Klein Tank, A.M.G., Klok, E.J., Jones, P.D., New, M., 2008. A European daily high-resolution gridded data set of surface temperature and precipitation for 1950–2006. *J. Geophys. Res.* 113, D20119. <https://doi.org/10.1029/2008JD010201>.
- Heide, O.M., 1993. Daylength and thermal time responses of budburst during dormancy release in some northern deciduous trees. *Physiol. Plant.* 88, 531–540. <https://doi.org/10.1111/j.1399-3054.1993.tb01368.x>.
- Hicks, S., Helander, M., Heino, S., 1994. Birch pollen production, transport and deposition for the period 1984–1993 at Kevo, northernmost Finland. *Aerobiologia (Bologna)* 10, 183–191. <https://doi.org/10.1007/BF02459234>.
- Hijmans, R.J., van Etten, J., 2014. *Raster: Geographic Data Analysis and Modeling*.
- Hirst, J.M., 1952. An automatic volumetric spore trap. *Ann. Appl. Biol.* 39, 257–265. <https://doi.org/10.1111/j.1744-7348.1952.tb00904.x>.
- Jato, V., Rodríguez-Rajo, F.J., Méndez, J., Aira, M.J., 2002. Phenological behaviour of Quercus in Ourense (NW Spain) and its relationship with the atmospheric pollen season. *Int. J. Biometeorol.* 46, 176–184. <https://doi.org/10.1007/s00484-002-0132-4>.
- Kramer, K., 1994. Selecting a model to predict the onset of growth of Fagus sylvatica. *J. Appl. Ecol.* 31, 172. <https://doi.org/10.2307/2404609>.
- Laaidi, M., 2001. Forecasting the start of the pollen season of Poaceae: evaluation of some methods based on meteorological factors. *Int. J. Biometeorol.* 45, 1–7. <https://doi.org/10.1007/s004840000079>.
- Lang, G.A., Early, J.D., Martin, G.C., Darnell, R.L., 1987. Endo, para-and ecodormancy: physiological terminology and classification for dormancy research. *HortScience* 371–377.
- Linkosalo, T., Ranta, H., Oksanen, A., Siljamo, P., Luomajoki, A., Kukkonen, J., Sofiev, M., 2010. A double-threshold temperature sum model for predicting the flowering duration and relative intensity of Betula pendula and B. pubescens. *Agric. For. Meteorol.* 150, 1579–1584. <https://doi.org/10.1016/j.agrformet.2010.08.007>.
- Myking, T., Heide, O.M., 1995. Dormancy release and chilling requirement of buds of latitudinal ecotypes of Betula pendula and B. pubescens. *Tree Physiol.* 15, 697–704. <https://doi.org/10.1093/treephys/15.11.697>.
- Nelder, J.A., Mead, R., 1965. A simplex method for function minimization. *Comput. J.* 7, 308–313. <https://doi.org/10.1093/comjnl/7.4.308>.
- Nilsson, S., Persson, S., 1981. Tree pollen spectra in the Stockholm region (Sweden), 1973–1980. *Grana* 20, 179–182. <https://doi.org/10.1080/00173138109427661>.
- Oteros, J., Bergmann, K.-C., Menzel, A., Damialis, A., Traidl-Hoffmann, C., Schmidt-Weber, C., Buters, J., 2018. Spatial interpolation of current airborne pollen concentrations where no monitoring exists. *Atmos. Environ.* <https://doi.org/10.1016/j.atmosenv.2018.11.045>.
- Pebesma, E., Bivand, R.S., 2005. *Classes and methods for spatial data: the sp package*. *R News*. vol. 5, pp. 9–13.
- Pfaar, O., Bastl, K., Berger, U., Buters, J., Calderon, M.A., Clot, B., Darsow, U., Demoly, P., Durham, S.R., Galán, C., Gehrig, R., Gerth van Wijk, R., Jacobsen, L., Klimek, L., Sofiev, M., Thibaudon, M., Bergmann, K.C., 2017. Defining pollen exposure times for clinical trials of allergen immunotherapy for pollen-induced rhinoconjunctivitis – an EAACI position paper. *Allergy Eur. J. Allergy Clin. Immunol.* 72, 713–722. <https://doi.org/10.1111/all.13092>.
- Recio, M., Picornell, A., Trigo, M.M., Gharbi, D., García-Sánchez, J., Cabezo, B., 2018. Intensity and temporality of airborne Quercus pollen in the southwest Mediterranean area: correlation with meteorological and phenoclimatic variables, trends and possible adaptation to climate change. *Agric. For. Meteorol.* 250–251, 308–318. <https://doi.org/10.1016/j.agrformet.2017.11.028>.
- Rodríguez-Rajo, F.J., Frenguelli, G., Jato, M.V., 2003. Effect of air temperature on forecasting the start of the Betula pollen season at two contrasting sites in the south of Europe (1995–2001). *Int. J. Biometeorol.* 47, 117–125. <https://doi.org/10.1007/s00484-002-0153-z>.
- Rojo, J., Picornell, A., Oteros, J., 2019. AeRobiology: the computational tool for biological data in the air. *Methods Ecol. Evol.* 1–6. <https://doi.org/10.1111/2041-210X.13203>.
- Skjøth, C.A., Sommer, J., Stach, A., Smith, M., Brandt, J., 2007. The long-range transport of birch (Betula) pollen from Poland and Germany causes significant pre-season concentrations in Denmark Clinical and Experimental Allergy. *Clin. Exp. Allergy*, 1204–1212. <https://doi.org/10.1111/j.1365-2222.2007.02771.x>.
- Sofiev, M., Galperin, M., Genikhovich, E., 2008. A construction and evaluation of Eulerian dynamic core for the air quality and emergency modelling system SILAM. *Air Pollution Modeling and Its Application XIX*. Springer, Netherlands, Dordrecht, pp. 699–701. https://doi.org/10.1007/978-1-4020-8453-9_94.
- Sofiev, M., Siljamo, P., Ranta, H., Linkosalo, T., Jaeger, S., Rasmussen, A., Rantio-Lehtimäki, A., Severova, E., Kukkonen, J., 2013. A numerical model of birch pollen emission and dispersion in the atmosphere. Description of the emission module. *Int. J. Biometeorol.* 57, 45–58. <https://doi.org/10.1007/s00484-012-0532-z>.
- Spiekma, F.T.M., Emberlin, J.C., Hjelmroos, M., Jäger, S., Leuschner, R.M., 1995. Atmospheric birch (Betula) pollen in Europe: trends and fluctuations in annual quantities and the starting dates of the seasons. *Grana* 34, 51–57. <https://doi.org/10.1080/00173139509429033>.
- Subba Reddi, C., Reddi, N.S., 2009. Relation of Pollen Release to Pollen Concentrations in Air. <https://doi.org/10.1080/00173138509429921>.
- Thomas, B., Vince-Prue, D., 1997. *Photoperiodism in Plants*. Second. Academic Press, London.
- Tormo-Molina, R., Gonzalo-Garijo, M.A., Silva-Palacios, I., Muñoz-Rodríguez, A.F., 2010. General trends in airborne pollen production and pollination periods at a Mediterranean site (Badajoz, Southwest Spain). *J. Investig. Allergol. Clin. Immunol.* 20 (7), 567–574.
- Tutin, T., Heywood, V., Burges, N., Valentine, D., Walters, S., 1964. *Flora Europaea*. The syndics of the Cambridge University Press, Cambridge. <https://doi.org/10.5281/ZENODO.302862>.
- Van Vliet, A.J.H., Overeem, A., De Groot, R.S., Jacobs, A.F.G., Spiekma, F.T.M., 2002. The influence of temperature and climate change on the timing of pollen. *Int. J. Climatol.* 22, 1757–1767. <https://doi.org/10.1002/joc.820>.
- VDI4252-4, 2016. *Bioaerosole und biologische Agenzien – Ermittlung von Pollen und Sporen in der Außenluft unter Verwendung einer volumetrischen Methode für ein Messnetz zu allergologischen Zwecken*. VDI-Richtlinie 4252 Blatt 4, Entwurf. VDI/DIN-Handbuch Reinhaltung der Luft, Band 1a. Beuth, Berlin.
- Vogel, B., Vogel, H., Bäumer, D., Bangert, M., Lundgren, K., Rinke, R., Stanelle, T., 2009. The comprehensive model system COSMO-ART – radiative impact of aerosol on the state of the atmosphere on the regional scale. *Atmos. Chem. Phys.* 9, 8661–8680. <https://doi.org/10.5194/acp-9-8661-2009>.
- Wickham, H., 2016. *ggplot2: Elegant Graphics for Data Analysis*. Springer International Publishing. <https://doi.org/10.1007/978-3-319-24277-4>.
- Willmott, C., Matsuura, K., 2005. Advantages of the mean absolute error (MAE) over the root mean square error (RMSE) in assessing average model performance. *Clim. Res.* 30, 79–82. <https://doi.org/10.3354/cr00799>.
- Winkler, H., Ostrowski, R., Wilhelm, M., Bergmann, K.C., 2001. *Pollenbestimmungsbuch der Stiftung. Takt*, Berlin.